Cage Compounds

International Edition: DOI: 10.1002/anie.201907432
German Edition: DOI: 10.1002/ange.201907432

Unconventional Metal–Framework Interaction in $MgSi_5$

Julia-Maria Hübner, Wilder Carrillo-Cabrera, Yurii Prots, Matej Bobnar, Ulrich Schwarz, and Yuri Grin*

Abstract: *The silicon-rich cage compound $MgSi_5$ was obtained by high-pressure high-temperature synthesis. Initial crystal structure determination by electron diffraction tomography provided the basis for phase analyses in the process of synthesis optimization, finally facilitating the growth of single crystals suitable for X-ray diffraction experiments. The crystal structure of $MgSi_5$ (space group Cmme, Pearson notation oS24, $a = 4.4868(2)$ Å, $b = 10.1066(5)$ Å, and $c = 9.0753(4)$ Å) constitutes a new type of framework of four-bonded silicon atoms forming Si_{15} cages enclosing the Mg atoms. Two types of smaller Si_8 cages remain empty. The atomic interactions are characterized by two-center two-electron bonds within the silicon framework. In addition, there is evidence for multicenter Mg–Si bonding in the large cavities of the framework and for lone-pair-like interactions in the smaller empty voids.*

Intermetallic framework compounds[1] constitute fascinating inorganic phases, in which a majority of framework atoms enclose a minority of guest species. In recent years, this class of materials attracted significant interest in preparative solid-state chemistry and current basic materials science research because several members exhibit beneficial thermoelectric or superconducting properties.[2] The structural organization covers a wide variety of compositions involving three-dimensional frameworks usually based on four-bonded tetrel atoms such as Si, Ge, or Sn. Generally, the connectivity of the network atoms is related to the electron count by the $8-N$ rule although silicon compounds may tolerate a certain electron excess.[3]

Typically, members of the alkaline, alkali-earth, or rare-earth metal groups act as cationic guest species. However, magnesium constitutes an exception as the metal tends to participate in the anionic network, for example, in TiNiSi-type CaMgSi or $BaAl_4$-type phases such as $EuGa_{4-x}Mg_x$.[4] At ambient pressure, the binary system Mg-Si shows (anti-)fluorite-type Mg_2Si as the only phase,[5] and also ternary magnesium–silicon compounds tend to evade clathrate-like frameworks.[4,6] However, high-pressure synthesis techniques provide valuable tools for advancing the spectrum of accessible tetrel frameworks regarding network topology and chemical composition.[7,8]

Herein, we report on the synthesis, crystal structure, and chemical bonding of a silicon framework embedding cationic magnesium in a binary compound. $MgSi_5$ was obtained by high-pressure synthesis between 5(1) and 10(1) GPa upon heating to temperatures between 1173(120) K and 1373(150) K and quenching to room temperature before decompression. At normal pressure, the diamagnetic compound decomposed at 468(10) K (see Figures S1 and S2 in the Supporting Information). The new compound was first discovered by scanning electron microscopy (SEM) in form of domains in matrices of *hp*-Mg_9Si_5 and (*cF*8)Si. Specimens suitable for selected area electron diffraction experiments were prepared by the focused ion beam (FIB) lift-out technique (Figure 1 and Figure S3). Manual electron diffraction tomography measurements yielded 354 reflections indicating the space group *Cmme*. Structure solution was performed using 142 symmetry-independent reflections (Tables S1 and S2).

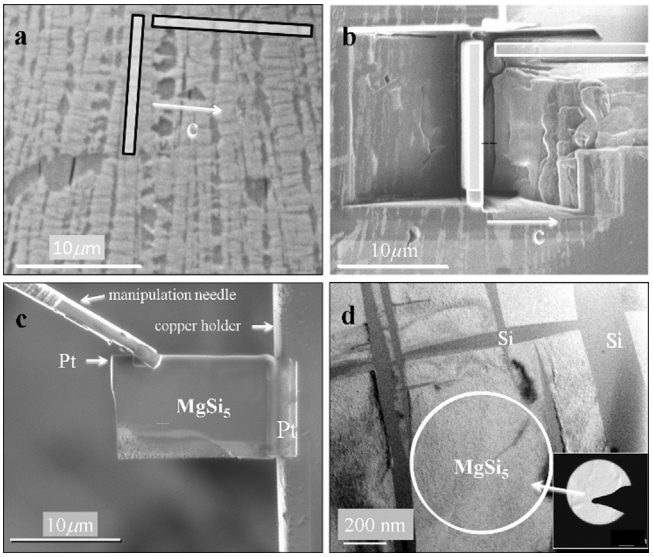

Figure 1. a) Polished surface of the $MgSi_5$ sample (back-scattering-electron scanning electron microscopy image) with arrays of equally oriented domains of $MgSi_5$ (light gray), separated by thin Si layers (dark gray); black frames show the positions of the FIB cuts. b) Surface image after extracting the first FIB cut. c) Second FIB cut soldered to the copper holder. d) Transmission electron microscopy image of a FIB lamella (perpendicular to [001]) showing the area used for electron diffraction tomography (circle). The inset shows the aperture.

[*] M. Sc. J.-M. Hübner, Dr. W. Carrillo-Cabrera, Dr. Yu. Prots, Dr. M. Bobnar, Dr. U. Schwarz, Prof. Yu. Grin
Chemische Metallkunde
Max-Planck-Institut für Chemische Physik fester Stoffe
Nöthnitzer Straße 40, 01187 Dresden (Germany)
E-mail: schwarz@cpfs.mpg.de
Supporting information and the ORCID identification number(s) for the author(s) of this article can be found under: https://doi.org/10.1002/anie.201907432.

The determination of basic crystallographic information and chemical composition set the stage for optimizing the synthesis conditions. Powder diffraction patterns with LaB_6 as an internal standard resulted in lattice parameters of $a =$ 4.4868(2) Å, $b = 10.1066(5)$ Å, and $c = 9.0753(4)$ Å. The optimized synthesis produced ingots containing specimen of sufficient size and quality for single crystal X-ray diffraction. These were isolated from the crude product by leaching with 0.1 M NaOH.

Structure refinement with single-crystal and powder X-ray diffraction data (Tables S3–S5) shows that $MgSi_5$ represents a new structure type (Pearson notation *oS*24; Figure 2). The crystal structure can be described as a three-dimensional framework of four-bonded (4*b*) Si atoms with Si_{15} cages centered by Mg atoms and empty Si_8 polyhedra (Figure 2a). The filled $[MgSi_{15}]$ cages are stacked along [100] and form columns by sharing pentagonal faces (Figure 2b). The stacking sequence in $MgSi_5$ resembles that of $LaSi_{10}$[9] and bears pronounced similarity to the arrangement of MSi_{18} polyhedra in the compounds MSi_6 (M = Ca, Sr, Ba, Eu).[7] The space between the columns is filled by empty Si_8 polyhedra—strongly distorted rhombic antiprisms—of two kinds A and B (Figure 2a,c,d). The connected $Si_{6/4}$ boat rings of the type A cavities (Figure 2c) resemble the proposed atomic arrangement of carbon atoms in sp^3 hydrocarbon (2,2) nanotubes.[10] The observed distances between 2.379(2) and 2.4742(8) Å between neighboring silicon atoms in $MgSi_5$ (Table S6) are longer than those observed in elemental Si (2.3516 Å[11]).

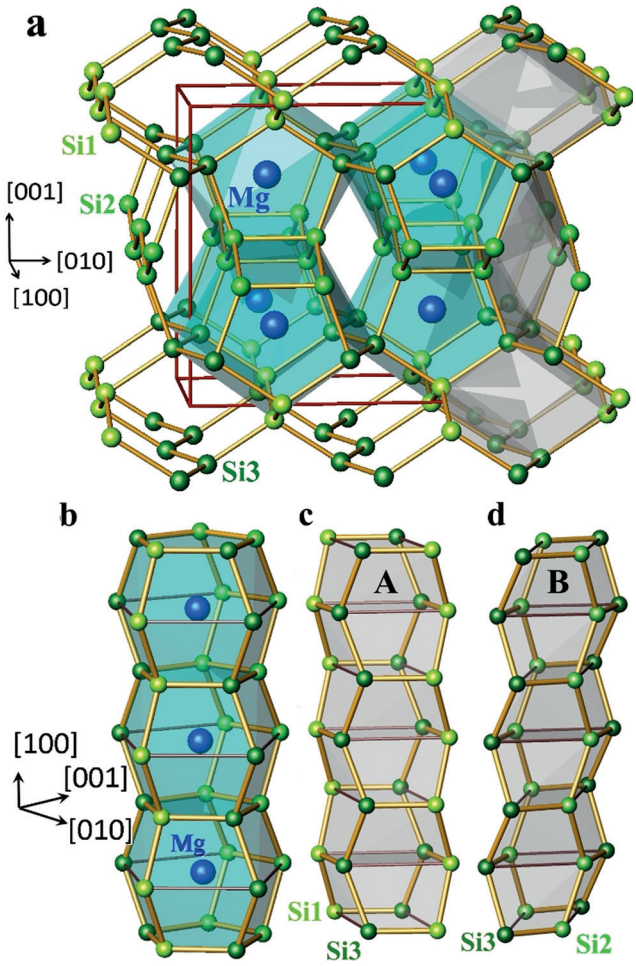

Figure 2. Crystal structure of $MgSi_5$: a) Short Si–Si distances indicated by golden lines emphasize the framework of four-bonded silicon atoms with Si_{15} cages ($[4^25^26^4]$, light-blue) centered by Mg atoms and two kinds of empty cages A and B (light gray). b) Columns of condensed centered $[MgSi_{15}]$ cages. c,d) Face-sharing empty Si_8 cages of types A and B, respectively.

According to the Zintl–Klemm concept and the $8-N$ rule, frameworks containing solely four-bonded tetrel atoms would not require additional electrons for stabilization. Thus, the electron balance of $MgSi_5$ with (4*b*)Si atoms may be written as $MgSi_5 = [Mg^{2+}][(4b)Si^0]_5 \times 2e^-$ with two excess electrons per formula unit. In a simple picture for a four-bonded silicon network with electron excess, the electronic density of states (DOS) below the Fermi level would consist of two ranges, which are dominated by s and p states of silicon, respectively, and above a pseudo-gap-like minimum, several anti-bonding states are populated. For example, Ba-containing clathrates show such a DOS pattern.[12] In comparison to that situation, the calculated electronic DOS for $MgSi_5$ reveals distinct differences (Figure 3a). First, the Si-s- and Si-p-dominated regions below the Fermi level can still be recognized by the corresponding atomic contributions, but there is no marked separation like the gap found for Ba clathrates.[3,12]

Second, the Fermi level is located almost exactly in the center of a pseudo-gap, again in contrast to a typical clathrate-like DOS. Such a situation may arise if "anti-bonding" states change character because of lone-pair-like configurations ("non-bonding" states) or direct (multi-center) interactions between silicon and magnesium (bonding states). In line with this picture, the integration of the electronic DOS in the window between −0.62 eV (first dip in the DOS below E_F) and the Fermi level yielded quite precisely two electrons per formula unit. These findings of the DOS analysis were used as the starting point for a detailed study of the chemical bonding in $MgSi_5$ by positional-space quantum-chemical techniques.

The electron density of $MgSi_5$ reveals magnesium species with an almost spherical shape, which according to the quantum theory of atoms in molecules (QTAIM[13]) indicates a mostly cationic character of the magnesium atoms (Figure 4). However, some characteristics of the distribution differ from that of typical cationic metal species, such as in clathrates.[12] Despite the generally convex surface, we note here that the faces in the (100) plane are significantly flattened, which hints at a distinct covalence of the interactions between magnesium and silicon. The effective QTAIM charge of +1.6 for Mg is in good agreement with the large electronegativity difference between Mg and Si. The corresponding charges in other intermetallic compounds of magnesium amount to values between +1.28 and +1.59;[14] the calculated results for $Mg_{1-x}B_2$ range from +1.4 to +1.6.[15] The shapes of the silicon species are more polyhedral-like, and the flat contact faces between neighboring atoms are typical for non-polar covalent bonding. The silicon QTAIM atoms have charges between 0.0 and −0.6, revealing an unequal charge transfer from the magnesium to the silicon atoms.

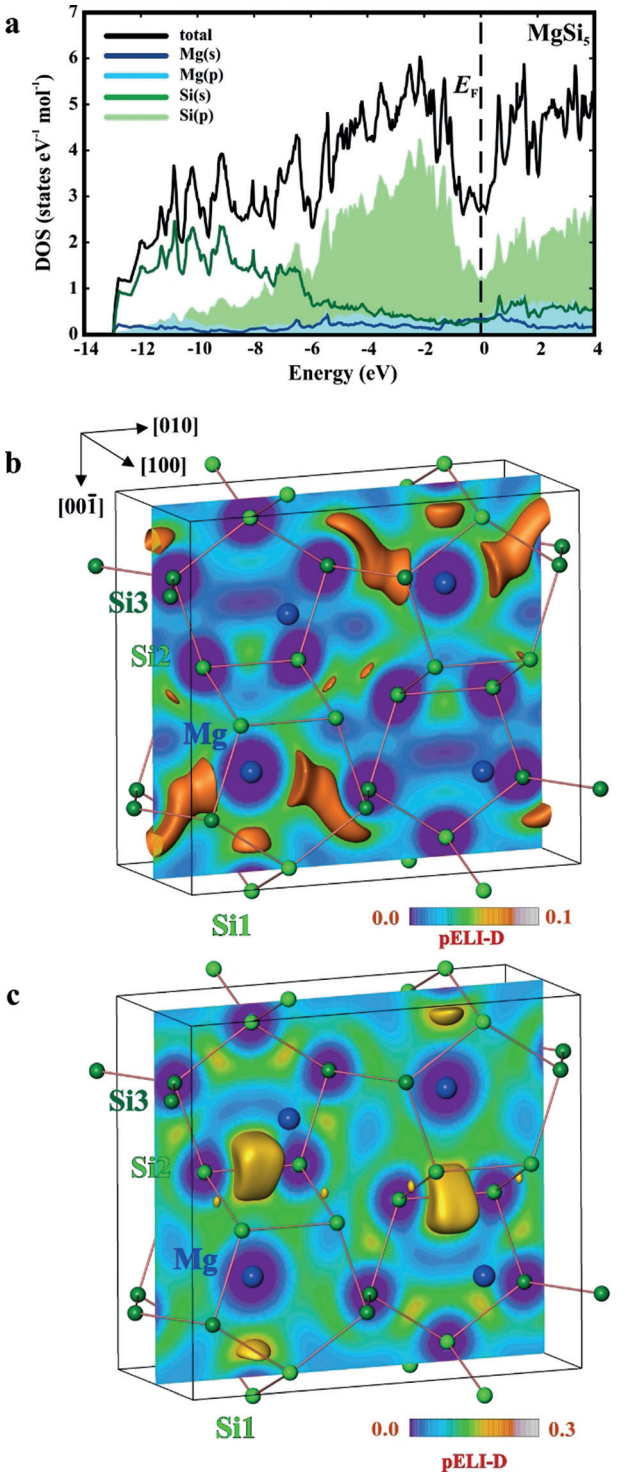

Figure 3. Electronic structure of and chemical bonding in $MgSi_5$: a) Total DOS and atomic contributions of Mg and Si. b) Distribution of partial ELI-D in the (200) plane and isosurface with pELI-D = 0.077 calculated for the energy window $-0.62\ eV \le E \le E_F$. c) Distribution of partial ELI-D in the (200) plane and isosurface with pELI-D = 0.166 for the energy range $-1.56\ eV \le E \le -0.62\ eV$.

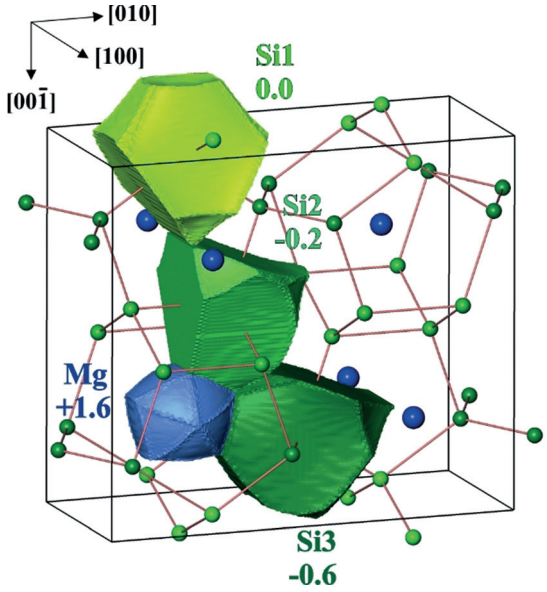

Figure 4. QTAIM atoms and their effective charges in $MgSi_5$.

The distribution of the electron localizability indicator (ELI-D) reveals the typical picture of four-bonded silicon atoms. The maxima visualized by the isosurface with ELI-D = 1.44 (Figure 5a–c) are located on or close to the bond lines between silicon atoms. Moreover, the corresponding basin populations of these attractors (Figure 5a) amount to values of around two electrons. The intersection of the atomic basins of magnesium with the bonding basins of the Si–Si bonds indicate only a small contribution of Mg to three-atom interactions, as suggested by the location of small parts of the Si–Si bonding basins within the atomic basin of Mg (Figure 5c). A new feature of the ELI-D appears in vicinity of the Si2 atoms within the cavity labeled B. The local ELI-D maximum reveals a lone-pair-like interaction between neighboring Si2 atoms in the (100) plane across the cavity. Although the population of 0.27 electrons for the according basin (light yellow in Figure 5b,c) is rather small, its presence is the first hint to additional interactions within the crystal structure. This is also suggested by an analysis of the electronic DOS.

In order to study this finding in more detail, the contributions of electrons in certain energy regions below the Fermi level were investigated by partial ELI-D (pELI-D).[16] The calculation for states with energies between −0.62 e (first dip in the DOS below E_F; Figure 3a) up to the Fermi level shows main pELI-D contributions close to the lone-pair-like attractor of Si2 in cavity B, confirming that this interaction is supported by magnesium electrons, which stabilize the cavity (Figure 3b). Further local maxima are found on the bond lines between Mg and Si2 and Si3, revealing multi-center Mg–Si interactions within the large cavity of the framework. Finally, large values are also observed within cavity A. Although the pELI-D values are insufficiently high to form a local maximum, they still suggest a polar—or a lone-pair-like—interaction. Both silicon atoms Si2 and Si3 acting within the small cavities have larger negative charges than Si1, which does not interact in the voids. The calculated pELI-D for the next energy window between −1.56 eV and −0.62 eV (Figure 3c) reveals mainly contribu-

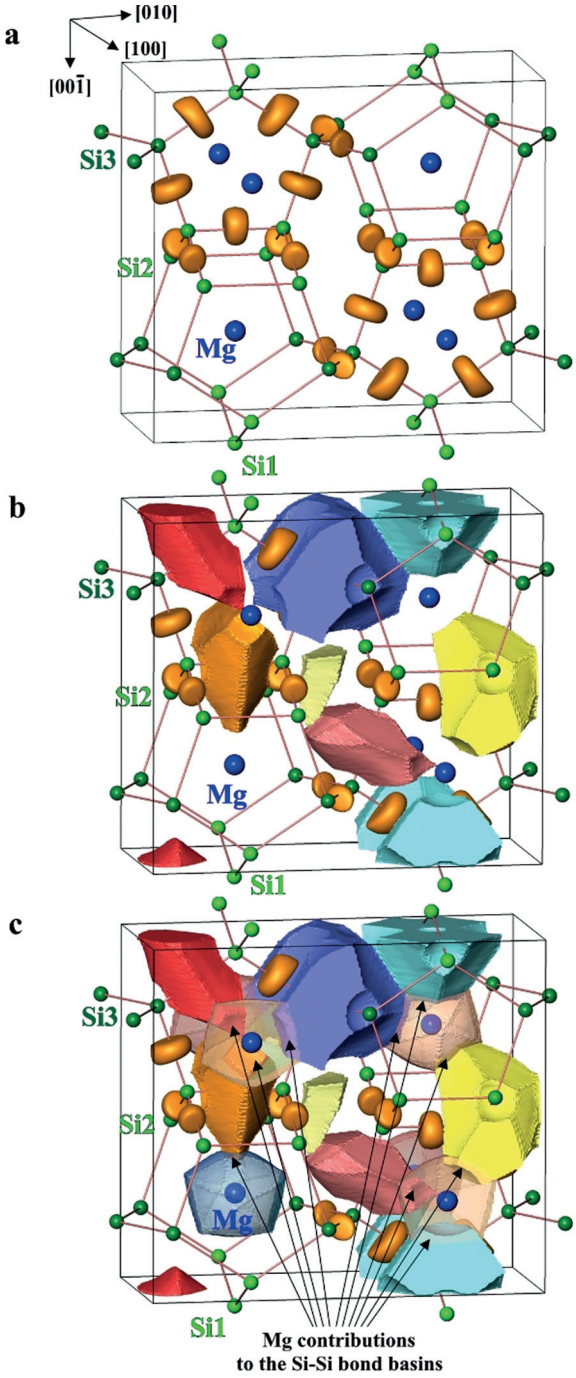

Figure 5. Electron localizability indicator in $MgSi_5$: a) Isosurface of ELI-D = 1.44 (orange disks). b,c) Bond basins Si1–Si3 (red), Si3–Si3 (dark blue), Si2–Si2 (orange), Si2–Si2 (yellow), Si1–Si1 (light blue), and Si2–Si3 (pink) plus the "lone pair" at Si2 (light yellow) together with their electronic populations. c) Overlap of the shapes of QTAIM Mg atoms (transparent pink) with the Si–Si bonding basins reveal only small contributions of the Mg atoms to the Si–Si interactions.

tions to Mg–Si1 and Si–Si bonding, characteristic for cage (clathrate-like) compounds.

In summary, the electronic structure of the silicon-rich cage compound $MgSi_5$ exhibits distinct differences to typical intermetallic host–guest assemblies despite similar structural features. The calculated electronic density of states of $MgSi_5$ reveals a clear pseudo-gap around the Fermi level. Chemical bonding is organized in form of conventional two-center two-electron bonds within the three-dimensional silicon framework. In addition, there is evidence for multi-atom bonding between framework and cage atoms in the large cavities as well as lone-pair-like interactions in the smaller empty voids of the framework.

Experimental Section

$MgSi_5$ was obtained by high-pressure, high-temperature synthesis between 5(1) and 10(1) GPa upon heating to temperatures between 1173(120) K and 1373(150) K before quenching to ambient conditions (see the Supporting Information). Thin samples prepared from crude ingots by the focused ion beam (FIB) lift-out technique[17] were investigated with transmission electron microscopy by means of selected area electron diffraction data for structure solution (see the Supporting Information).[18] Refinements of X-ray diffraction data were performed with the crystallographic program package WinCSD.[19] Electronic band structure calculations (Figure S4) and bonding analysis of $MgSi_5$ were carried out using the experimental values of lattice parameters and atomic coordinates (Tables S3 and S4) employing the program package TB-LMTO-ASA (see the Supporting Information).[20–22] Position-space analysis of the chemical bonding in $MgSi_5$ was performed by means of the electron localizability approach (see the Supporting Information).[16,23–26]

Acknowledgements

We thank Susann Leipe for supporting high-pressure syntheses, Marcus Schmidt and Susann Scharsach for DSC measurements, Ulrich Burkhardt, Sylvia Kostmann, and Petra Scheppan for metallographic characterizations as well as Gudrun Auffermann and Ulrike Schmidt for chemical analysis. Stimulating discussions with Frank R. Wagner are appreciated. J.-M.H. gratefully acknowledges support by the International Max Planck Research School for Chemistry and Physics of Quantum Materials.

Conflict of interest

The authors declare no conflict of interest.

Keywords: cage compounds · chemical bonding · high-pressure synthesis · magnesium · silicon

How to cite: *Angew. Chem. Int. Ed.* **2019**, *58*, 12914–12918
Angew. Chem. **2019**, *131*, 13046–13050

[1] a) M. Pouchard, C. Cros in *The Physics and Chemistry of Inorganic Clathrates* (Ed.: G. S. Nolas), Springer, Dordrecht, **2014**, pp. 1–33; b) M. Baitinger, B. Böhme, A. Ormeci, Yu. Grin in *The Physics and Chemistry of Inorganic Clathrates* (Ed.: G. S. Nolas), Springer, Dordrecht, **2014**, pp. 35–64; c) C. Cros, M. Pouchard, P. Hagenmüller, *J. Solid State Chem.* **1970**, *2*, 570–558; d) M. Beekman, G. S. Nolas, *J. Mater. Chem.* **2008**, *18*, 842–851; e) S. Yamanaka, *Dalton Trans.* **2010**, *39*, 1901–1915; f) A. V. Shevelkov, K. Kovnir, *Struct. Bonding (Berlin)* **2011**, *139*, 97–142; g) S. C. Peter, M. G. Kanatzidis, *Z. Anorg. Allg. Chem.* **2012**, *638*, 287–293; h) A. Iyo, I. Hase, K. Kawashima, S. Ishida, H.

Kito, N. Takeshita, K. Oka, H. Fujihisa, Y. Gotoh, Y. Yoshida, H. Eisaki, *Inorg. Chem.* **2017**, *56*, 8590 – 8595.
[2] a) S. Stefanoski, M. Beekman, G. S. Nolas in *The Physics and Chemistry of Inorganic Clathrates* (Ed.: G. S. Nolas), Springer, Dordrecht, **2014**, pp. 169 – 191; b) S. Yamanaka in *The Physics and Chemistry of Inorganic Clathrates* (Ed.: G. S. Nolas), Springer, Dordrecht, **2014**, pp. 193 – 226; c) J.-A. Dolyniuk, B. Owens-Baird, J. Wang, J. V. Zaikina, K. Kovnir, *Mater. Sci. Eng.* **2016**, *108*, 1 – 46; d) K. A. Kovnir, A. V. Shevelkov, *Russian Chem. Rev.* **2004**, *73*, 923 – 938; e) A. M. Guloy, J. D. Corbett, *Inorg. Chem.* **1991**, *30*, 4789 – 4794; f) F. Kneidinger, H. Michor, A. Sidorenko, E. Bauer, I. Zeiringer, P. Rogl, C. Blaas-Schenner, D. Reith, R. Podloucky, *Phys. Rev. B* **2013**, *88*, 104508.
[3] A. Bhattacharya, C. Carbogno, B. Böhme, M. Baitinger, Yu. Grin, M. Scheffler, *Phys. Rev. Lett.* **2017**, *118*, 236401.
[4] a) H. Axel, B. Eisenmann, H. Schäfer, A. Weiss, *Z. Naturforsch. B* **1969**, *24*, 815 – 817; b) B. Eisenmann, H. Schäfer, A. Weiss, *Z. Anorg. Allg. Chem.* **1972**, *391*, 241 – 254; c) F. Merlo, M. Pani, M. L. Fornasini, *J. Alloys Compd.* **1993**, *196*, 145 – 148; d) S. J. Andersen, C. D. Marioara, A. Froseth, R. Vissers, H. W. Zandbergen, *Mater. Sci. Eng. A* **2005**, *390*, 127 – 138; e) A. O. Fedorchuk, Yu. Prots, Yu. Grin, *Z. Kristallogr. New Cryst. Struct.* **2005**, *220*, 317 – 318.
[5] X. Y. Yan, Y. A. Chang, F. Zhang, *J. Phase Equilib.* **2000**, *21*, 379 – 384.
[6] a) H. Witte, *Metallwirtsch.* **1939**, *18*, 459 – 463; b) R. J. LaBotz, D. R. Mason, D. F. O'Kane, *J. Electrochem. Soc.* **1963**, *110*, 127 – 134; c) B. Eisenmann, N. May, W. Müller, H. Schäfer, A. Weiss, J. Winter, G. Ziegleder, *Z. Naturforsch. B* **1970**, *25*, 1350 – 1352; d) F. Wrubl, M. Pani, P. Manfrinetti, P. Rogl, *J. Solid State Chem.* **2009**, *182*, 716 – 724; e) A. Currao, J. Curda, R. Nesper, *Z. Anorg. Allg. Chem.* **1996**, *622*, 85 – 94; f) R. Nesper, S. Wengert, F. Zürcher, A. Currao, *Chem. Eur. J.* **1999**, *5*, 3382 – 3389; g) I. Schellenberg, M. Eul, C. Schwickert, C. M. Kubata, E. C. Reyes, R. Nesper, U. C. Rodewald, R. Pöttgen, *Z. Anorg. Allg. Chem.* **2012**, *638*, 1976 – 1985.
[7] a) S. Yamanaka, S. Maekawa, *Z. Naturforsch. B* **2006**, *61*, 1493 – 1499; b) A. Wosylus, Yu. Prots, U. Burkhardt, W. Schnelle, U. Schwarz, Yu. Grin, *Z. Naturforsch. B* **2006**, *61*, 1485 – 1492; c) A. Wosylus, Yu. Prots, U. Burkhardt, W. Schnelle, U. Schwarz, *Sci. Technol. Adv. Mater.* **2007**, *8*, 383 – 388; d) A. Wosylus, Yu. Prots, U. Burkhardt, W. Schnelle, U. Schwarz, Yu. Grin, *Solid State Sci.* **2006**, *8*, 773 – 781.
[8] a) H. Fukuoka, S. Yamanaka, *Phys. Rev. B* **2003**, *67*, 094501; b) U. Schwarz, A. Wosylus, H. Rosner, W. Schnelle, A. Ormeci, K. Meier, A. Baranov, M. Nicklas, S. Leipe, C. J. Müller, Yu. Grin, *J. Am. Chem. Soc.* **2012**, *134*, 13558 – 13561.
[9] S. Yamanaka, S. Izumi, S. Maekawa, K. Umemoto, *J. Solid State Chem.* **2009**, *182*, 1991 – 2003.
[10] D. Stojkovic, P. Zhang, V. H. Crespi, *Phys. Rev. Lett.* **2001**, *87*, 125502.
[11] W. M. Yim, R. J. Paff, *J. Appl. Phys.* **1974**, *45*, 1456 – 1457.
[12] A. Ormeci, Yu. Grin, *J. Thermoelectr.* **2015**, *6*, 16 – 32.
[13] R. F. W. Bader, *Atoms in molecules: A quantum theory*, Oxford University Press, Oxford, **1999**.
[14] a) R. Pöttgen, V. Hlukhyy, A. Baranov, Yu. Grin, *Inorg. Chem.* **2008**, *47*, 6051 – 6055; b) A. M. Alekseeva, A. Leithe-Jasper, Yu. Prots, W. Schnelle, A. Ormeci, E. V. Antipov, Yu. Grin, *Chem. Met. Alloys* **2014**, *7*, 74 – 84; c) A. M. Alekseeva, A. M. Abakumov, A. Leithe-Jasper, W. Schnelle, Yu. Prots, G. Van Tendeloo, E. V. Antipov, Yu. Grin, *Chem. Eur. J.* **2013**, *19*, 17860 – 17870.
[15] V. Tsirelson, A. Stash, M. Kohout, H. Rosner, H. Mori, S. Sato, S. Lee, A. Yamamoto, S. Tajima, Yu. Grin, *Acta Crystallogr. Sect. B* **2003**, *59*, 575 – 583.
[16] F. R. Wagner, V. Bezugly, M. Kohout, Yu. Grin, *Chem. Eur. J.* **2007**, *13*, 5724 – 5741.
[17] Z. Wang, W. Wan, J. Sun, W. Carrillo-Cabrera, D. Grüner, X. Yin, S. Qiu, G. Zhu, X. Zou, *CrystEngComm* **2012**, *14*, 2204 – 2212.
[18] a) U. Kolb, E. Mugnaioli, T. E. Gorelik, *Cryst. Res. Technol.* **2011**, *46*, 542 – 554; b) V. Petříček, M. Dušek, L. Palatinus, *Z. Kristallogr.* **2014**, *229*, 345 – 352.
[19] L. Akselrud, Yu. Grin, *J. Appl. Crystallogr.* **2014**, *47*, 803 – 805.
[20] O. Jepsen, A. Burkhardt, O. K. Andersen, The Program TB-LMTO-ASA. Version 4.7. Max-Planck-Institut für Festkörperforschung, Stuttgart, **1999**.
[21] U. von Barth, L. Hedin, *J. Phys. C* **1972**, *5*, 1629 – 1642.
[22] O. K. Andersen, *Phys. Rev. B* **1975**, *12*, 3060 – 3083.
[23] a) M. Kohout, *Int. J. Quantum Chem.* **2004**, *97*, 651 – 658; b) M. Kohout, *Faraday Discuss.* **2007**, *135*, 43 – 54.
[24] M. Kohout, DGrid, versions 4.6 – 5.0, **2018**.
[25] a) M. Kohout, A. Savin, *Int. J. Quantum Chem.* **1996**, *60*, 875 – 882; b) Yu. Grin, in *Comprehensive Inorganic Chemistry II*, *Vol. 2*, Elsevier, Oxford, **2013**. p. 359 – 373; c) Yu. Grin, A. Savin, B. Silvi, *The Chemical Bond: Chemical Bonding Across the Periodic Table*, Wiley-VCH, Weinhiem, **2014**, pp. 345 – 382.
[26] a) D. Bende, F. R. Wagner, Yu. Grin, *Inorg. Chem.* **2015**, *54*, 3970 – 3978; b) F. R. Wagner, R. Cardoso-Gil, B. Boucher, M. Wagner-Reetz, J. Sichelschmidt, P. Gille, M. Baenitz, Yu. Grin, *Inorg. Chem.* **2018**, *57*, 12908 – 12919; c) R. Freccero, P. Solokha, S. De Negri, A. Saccone, Yu. Grin, F. R. Wagner, *Chem. Eur. J.* **2019**, *25*, 6600 – 6612.

Manuscript received: June 14, 2019
Accepted manuscript online: July 24, 2019
Version of record online: August 19, 2019

